

Published in final edited form as:

*J Physiol Paris*. 2014 February ; 108(1): 28–37. doi:10.1016/j.jphysparis.2013.07.002.

## A Biologically Inspired Hierarchical Goal Directed Navigation Model

Uğur M. Erdem\* and Michael E. Hasselmo

Center for Memory and Brain and Graduate Program for Neuroscience, Boston University, 2 Cummings Mall, Boston, MA 02215, USA

Michael E. Hasselmo: hasselmo@bu.edu

### Abstract

We propose an extended version of our previous goal directed navigation model based on forward planning of trajectories in a network of head direction cells, persistent spiking cells, grid cells, and place cells. In our original work the animat incrementally creates a place cell map by random exploration of a novel environment. After the exploration phase, the animat decides on its next movement direction towards a goal by probing linear look-ahead trajectories in several candidate directions while stationary and picking the one activating place cells representing the goal location. In this work we present several improvements over our previous model. We improve the range of linear look-ahead probes significantly by imposing a hierarchical structure on the place cell map consistent with the experimental findings of differences in the firing field size and spacing of grid cells recorded at different positions along the dorsal to ventral axis of entorhinal cortex. The new model represents the environment at different scales by populations of simulated hippocampal place cells with changing firing field sizes. Among other advantages this model allows simultaneous constant duration linear look-ahead probes at different scales while significantly extending each probe range. The extension of the linear look-ahead probe range while keeping its duration constant also limits the degrading effects of noise accumulation in the network. We show the extended model's performance using an animat in a large open field environment.

### Keywords

grid cell; place cell; hippocampus; entorhinal cortex; navigation

## 1. INTRODUCTION

One of the crucial features of many living organisms capable of locomotion is their ability to navigate from their current location to another one to perform a life critical task. For instance squirrels are surprisingly good at rediscovering locations of food they previously buried (Jacobs and Liman, 1991), rats can learn to revisit or to avoid previously visited food locations (Brown, 2011; Olton and Schlosberg, 1978). Many animals retreat to a previously visited shelter in the presence of an immediate threat, e.g., a rabbit running to the safety of

---

© 2013 Elsevier Ltd. All rights reserved.

\*Corresponding author. merdem@bu.edu (Uğur M. Erdem).

**Publisher's Disclaimer:** This is a PDF file of an unedited manuscript that has been accepted for publication. As a service to our customers we are providing this early version of the manuscript. The manuscript will undergo copyediting, typesetting, and review of the resulting proof before it is published in its final citable form. Please note that during the production process errors may be discovered which could affect the content, and all legal disclaimers that apply to the journal pertain.

its burrow when it detects a bird of prey in the skies, or of a long-term threat, e.g., a bear retreating to a cave for hibernation to conserve energy during a cold season. It is a plausible assumption that for the organisms to perform such navigation tasks they should possess a cognitive mechanism to represent their environment as a collection of critical regions, e.g., nest locations, food locations, etc., to recall these regions when the need arises, and means to exploit relations between such regions (O'Keefe and Nadel, 1978; Redish, 1999).

The entorhinal cortex and hippocampus play a role in goal-directed behavior towards recently learned spatial locations in an environment. Rats show impairments in finding the spatial location of a hidden platform in the Morris water-maze after lesions of the hippocampus (Morris et al., 1982; Steele and Morris, 1999), postsubiculum (Taube et al., 1992) or entorhinal cortex (Steffenach et al., 2005). Recordings from these brain areas in behaving rats show neural spiking activity relevant to goal-directed spatial behavior, including grid cells in the entorhinal cortex that fire when the rat is in a repeating regular array of locations in the environment falling on the vertices of tightly packed equilateral triangles (Hafting et al., 2005; Moser and Moser, 2008). Experimental data also show place cells in the hippocampus that respond to mostly unique spatial locations (O'Keefe, 1976; McNaughton et al., 1983; O'Keefe and Burgess, 2005), head direction cells in the postsubiculum that respond to narrow ranges of allocentric head direction (Taube et al., 1990; Taube and Bassett, 2003), and cells that respond to translational speed of running (Sharp, 1996; O'Keefe et al., 1998).

In a previous work we proposed a goal-directed navigation model (Erdem and Hasselmo, 2012), inspired by experimental in-vivo findings, using a network of simulated head direction cells, grid cells, and place cells. The model represents each salient spatial location with the firing field of a place cell as the simulated subject (animat) explores its environment. During navigation the model guides the animat from an arbitrary location towards a previsited goal location by sampling potential linear look-ahead trajectory probes and picking the one which activates the place cell representing the desired location, i.e., the goal place cell. In this model all place cell firing fields are the same size and thus they represent the environment at a single scale. However, the model has some shortcomings. The noise accumulation during each look-ahead trajectory scan (collection of probes during a single look-ahead session) limits the duration and range of each look-ahead trajectory probe. Hence there is no guarantee that any of the probes will reach the goal place cell's firing field. Furthermore, if the radial distribution of the probes is not dense enough the look-ahead trajectory scan might still fail to activate the goal place cell even if the goal place field is in the probe range.

In this paper we present a navigation model which has significant extensions and improvements over our previously reported navigation model in Erdem and Hasselmo (2012). The model presented here tackles the problem of noise accumulation during linear look-ahead scan phase by representing the environment in a hierarchy of multiple scales. The hierarchical approach indirectly helps limiting the critical noise accumulation during look-ahead scans to acceptable levels. The extended model achieves noise stabilization by keeping the duration of a linear look-ahead trajectory probe, a critical component of the navigation system, constant while extending its range arbitrarily. We also report several other improvements over our previous single scale model.

The hierarchical approach to represent the environment in multiple scales is also supported by experimental in-vivo recordings. Differences in the firing field size and spacing of grid cells along the dorsal to ventral axis of entorhinal cortex have been reported in previous studies (Hafting et al., 2005; Sargolini et al., 2006; Giocomo et al., 2011). Grid cell firing field size and separation grows larger as the anatomical location of the cell slides from

dorsal to ventral border of entorhinal cortex. Also, CA3 place cell firing fields ranging from < 1 meter to 10 meters along the dorsal to ventral pole have been previously recorded (Kjelstrup et al., 2008; Jung and Wiener, 1994; Maurer et al., 2005). Both findings encourage the idea of hierarchical multi-scale representation of space in rats.

Our model of goal directed navigation based on spatial behavior of grid cells is also suited as a biologically-inspired model for SLAM (Simultaneous Localization And Mapping) in robotic navigation (Milford et al., 2004; Eustice et al., 2006; Guanella et al., 2007; Milford, 2008; Fible et al., 2010; Duff et al., 2011). However, none of the cited previous work exploits the advantages of a hierarchical approach.

## 2. MATERIAL AND METHODS

In this section we present the main ideas and constructs used to extend our previous goal-directed navigation model of linear look-ahead trajectories. We start by briefly explaining our original navigation model involving a network of the head direction cells, grid cells, and place cells as shown in Fig. 1. We show how this network is able to cognitively represent an explored environment as a place cell map. We continue by showing how linear look-ahead trajectory scans can be used to discover the best heading from the current location of the animat towards a predefined goal location. We then introduce our new model extending the previous one by using a hierarchical approach. This extended model represents a given environment using multiple place cell maps at different resolutions.

### 2.1. Notation

We show scalar parameters by italic lowercase characters, e.g.,  $a$ . Vectors are shown by bold lowercase characters, e.g.,  $\mathbf{a}$ . Vectors are row-wise unless specified otherwise. Matrices are shown by uppercase bold letter, e.g.,  $\mathbf{A}$ . We show an item's position index in a collection with subscripts, e.g.,  $a_i$ . Superscript is reserved for power operations with the exception of the transpose operation, e.g.,  $\mathbf{a}^T$ . We show collections such as sets and populations by uppercase italic letters, e.g.,  $A$ . Lowercase italic bold characters represent the class of the item they refer to, e.g., place cell  $\mathbf{p}$  or grid cell  $\mathbf{g}$ .

### 2.2. Single Level Place Cell Map

In our previous work we proposed a single scale model to solve the goal directed navigation task using a network of simulated head-direction cells tuned towards specific allocentric orientations using cosine tuning, entorhinal persistent spiking cells, entorhinal grid cells, hippocampal place cells, and pre-frontal cortical columns. Our original model works as explained briefly next.

**2.2.1. Head Direction Cells**—A head direction cell is a type of neuron tuned to increase its firing rate whenever the head direction (heading) of the animat gets closer to the cell's *preferred angle* (Taube et al., 1990). Extensive experimental data describe head direction cells in the deep layers of the entorhinal cortex (Sargolini et al., 2006) and in other areas including the postsubiculum (Taube et al., 1990). Previous work has also shown that usually a population of head direction cells are anchored to a salient landmark cue. In light of these, assuming that the firing rate of a head direction cell is cosine tuned and velocity modulated, we can represent its firing rate as follows:

$$\mathbf{D} = \begin{bmatrix} \cos(\theta_i + \theta_0) \dots \cos(\theta_m + \theta_0) \\ \sin(\theta_i + \theta_0) \dots \sin(\theta_m + \theta_0) \end{bmatrix} \quad (1a)$$

$$\mathbf{d}(t) = \mathbf{v}(t) \cdot \mathbf{D} = [d_1(t), \dots, d_m(t)] \quad (1b)$$

where  $\theta_i$  is the  $i^{\text{th}}$  cell's preferred angle,  $\theta_0$  is the heading angle of the anchor cue,  $\mathbf{D}$  is the tuning kernel,  $\mathbf{d}(t)$  is the vector of head direction firing rates at time  $t$ ,  $\mathbf{v}(t)$  is the animal's velocity vector at time  $t$ , and  $m$  is the total number of head direction cells in the model. All angles are allocentric, i.e., in the global coordinate system.

**2.2.2. Grid Cells**—A grid cell is a type of neuron tuned to fire whenever the animal's spatial position falls into regions of space, or *firing fields*, forming a periodic hexagonal grid pattern. Previous work have shown existence of grid cells showing firing fields with different inter-field spacing and firing field diameters (Hafting et al., 2005; Sargolini et al., 2006; Giocomo et al., 2011). Several computational models have previously been proposed to explain the grid cell mechanism. In our work we chose to use the *persistent spiking cell model* which falls into the category of *phase interference models* (Burgess et al., 2007; Burgess, 2008; Hasselmo, 2008). In standard slice preparations, most cortical neurons generate spikes during depolarizing input, but will not continue firing after stimulation ends. However, in the presence of cholinergic or metabotropic glutamate agonists, pyramidal cells in medial entorhinal cortex commonly show persistent firing (Klink and Alonso, 1997; Egorov et al., 2002; Fransen et al., 2006; Tahvildari et al., 2007; Yoshida et al., 2008) even when all synaptic input is blocked. The mechanisms of intrinsic persistent firing in single neurons could contribute to persistent spiking shown with unit recording during the delay period of delayed matching to sample tasks in awake, behaving rats (Young et al., 1997) and monkeys (Suzuki et al., 1997). Persistent spiking could also underlie persistent fMRI activation appearing during delay periods in human memory tasks, which can be reduced by muscarinic cholinergic blockade (Schon et al., 2004, 2005; Hasselmo and Stern, 2006). More detailed treatment of the grid cell model based on the interaction of persistent spiking cells can be found in Hasselmo (2008). The phase interference models explain the formation of periodic firing field grid as the result of interference between several oscillations with different frequencies. In the persistent spiking cell model each grid cell receives input from a set of persistent spiking cells. A persistent spiking cell generates a periodic spiking output. The frequency of this output is modulated by a head direction cell. The model is as follows:

$$\phi_{(i,j)}(t) = 2\pi \left( ft + b_j \int_0^t d_i(\tau) d\tau \right) \quad (2a)$$

$$s_{(i,j)}(t) = H(\cos(\phi_{(i,j)}(t) + \psi_{(i,j)}) - s_{thr}) \quad (2b)$$

$$g_j(t) = \prod_{s \in S_j} s(t) \quad (2c)$$

where  $\phi_{(i,j)}$  is the persistent spiking cell's phase modulated by the  $i^{\text{th}}$  head direction cell and projecting to the  $j^{\text{th}}$  grid cell,  $f$  is the frequency,  $b_j$  is the scaling factor for all persistent spiking cells projecting to  $j^{\text{th}}$  grid cell,  $s_{(i,j)}$  is the persistent spiking cell signal,  $\psi$  is the phase offset,  $s_{thr}$  is the threshold,  $H$  is the Heaviside function with  $H(0) = 0$ ,  $g$  is the grid cell signal, and  $S_j$  is the set of persistent spiking cells projecting to the  $j^{\text{th}}$  grid cell. A detailed coverage of each parameter is given in Erdem and Hasselmo (2012).

**2.2.3. Place Cells**—A place cell is a type of hippocampal neuron tuned to fire at specific, almost unique, locations in a given environment (O'Keefe, 1976). We model a place cell as a coincidence detector of action potential inputs converging from several grid cells:

$$p_k(t) = \prod_{g \in G_k} g(t) \quad (3)$$

where  $p_k$  is the  $k^{\text{th}}$  place cell signal and  $G_k$  is the set of grid cells projecting to the  $k^{\text{th}}$  place cell. It is important to note that the animat's spatial location is encoded by the *continuous* and *periodic* phase space of the persistent spiking cells while place cells generate action potentials at discrete regions of the phase space and the environment.

**2.2.4. Reward Cells**—A reward cell is a theoretical neuron representing the reward value associated with a place cell. Each place cell is bijectively connected to a reward cell. A reward cell is the simplified version of a pre-frontal cortex column presented in Erdem and Hasselmo (2012). In our navigation model, reward cells play a crucial role during the navigation towards a goal but not during random exploration. In the current version of our model a reward cell generates persistent spiking output whenever its associated place cell is a goal location:

$$r_k(t) = \begin{cases} 1 & \text{if } p_k \text{ is a goal location} \\ 0 & \text{otherwise} \end{cases} \quad (4)$$

where  $r_k$  is the output of the reward cell connected to the  $k^{\text{th}}$  place cell.

### 2.3. Linear Look Ahead Trajectory

The navigation task involves two phases: A random exploration phase and a goal-directed navigation phase. During the random exploration phase the animat cognitively encodes discrete regions of the environment as the firing fields of place cells. The question of when to represent a location by a place cell is still an open and very interesting question. In our work the time between two consecutive place cell recruitment is drawn from an exponential distribution parameterized by a rate parameter. The collection of place cells recruited during exploration forms the hippocampal representation of the explored environment as a *place cell map*. In the second phase of the navigation task the animat initially decides to navigate to a previously visited location represented by some place cell  $p_{goal}$ . The respective reward cell  $r_{goal}$  starts generating persistent spikes showing the animat's intended goal location (a goal location is associated with a reward) in the place cell map. Then the animat probes several candidate directions, Fig. 2, by forward linear look-ahead trajectories while stationary in one location. Each probe engages the head direction  $\rightarrow$  persistent spiking cell  $\rightarrow$  grid cell  $\rightarrow$  place cell network the same way as during free roaming but in a faster timescale. At the end of a full scan the animat selects the probe heading  $\theta_{goal}$  which activated the place cell  $p_{goal}$  and moves along heading  $\theta_{goal}$ . When the animat reaches the firing field of  $p_{goal}$  the goal-directed navigation phase and the navigation task ends.

Note that the original version of the goal-directed navigation model proposed in Erdem and Hasselmo (2012) involves an additional step where an exponentially decaying reward signal propagates across the reward cells following a connectivity topology established during the exploration phase. The decaying reward signal propagation creates a sparse gradient field in the reward cell network with its peak centered at the goal location. This reward gradient field serves two main purposes: i) It allows the goal-directed navigation phase to succeed even when the goal location is out of range of the forward linear look-ahead probes. The animat picks the heading of the probe activating the reward cell with maximum reward signal among all other reward cells activated during the full scan. ii) It allows the exploitation of never before experienced short-cuts towards the goal location.

Nevertheless, the original single level approach of Erdem and Hasselmo (2012) has several restrictions affecting the overall performance of the navigation task. In this paper we alleviate these restrictions by using a hierarchical place cell map representing the environment at different scales.

## 2.4. Hierarchical Place Cell Map

The three important limitations of the single level model are as follows:

1. In the absence of reward diffusion the success of the navigation task depends on the linear look-ahead probe range. If the goal place cell is not in the range of any probe during a full scan no probe will be able to activate any goal place cell. Without any heading towards goal location to pick the animat will fall back to random exploration. Unfortunately, increasing the probe range is not feasible. First, the amount of time that the animat can spend for a full scan is limited from above by a maximum value. Second, as the probe duration increases the noise accumulation degrades the accuracy of the probe. Degraded probe accuracy might generate false headings as the correct ones. The noise accumulation is expected to be a serious problem especially during the linear look-ahead scanning phase due to the absence of other sensory input modes, e.g., visual, that are available during normal navigation and can be used to correct for the excessive noise drift.
2. The angular arclength subtended between two consecutive probes becomes larger as the length of the probes increases. Since the place cell firing field size is constant in the single level approach, the probability of a probe to activate the goal place cell decreases with the probe length even if the goal place cell is in the range of a full scan. Decreasing the angle between neighboring probes increases the probability of activating the goal place cell but it also increases the number of probes and equivalently the duration of a full scan which takes us back to the first item.
3. Reward diffusion alleviates restrictions presented in items one and two. Unfortunately, the effective reward diffusion radius is also limited due to the signal decay at each hop between reward cells. After a certain number of hops the signal fidelity decreases to the cell's inherent noise levels hence providing no information for the linear look-ahead scan process.

In order to overcome these limitations, we propose a model with multiple place cell maps each representing the environment at a different scale as seen in experimental data by Kjelstrup et al. (2008). We augment the original notation of the single level model by representing the persistent spiking cell, the grid cell, and the place cell belonging to level  $l$  of the hierarchy as  $s_{(i,j,l)}$ ,  $\mathbf{g}_{(j,l)}$ , and  $\mathbf{p}_{(k,l)}$ . Other subscripts found in Eqn. 2 and in Eqn. 3 also change following the same logic. The scale of level  $l$  is parameterized by the scaling factor  $a_l$  of the augmented Eqn. 2a:

$$\phi_{(i,j,l)}(t) = 2\pi \left( ft + a_l b_j \int_0^t d_i(\tau) d\tau \right) \quad (5)$$

The scale parameter  $a_l$  is inversely proportional to the firing field radius,  $\rho_l$ , of place cell  $\mathbf{p}_{(k,l)}$ . Given the place cell firing field radius  $\rho_0$  of the highest resolution level 0 and  $\alpha$  being the relative scaling between two consecutive levels, the following hold:

$$a_l = \alpha^{-1} \rightarrow \frac{a_{(l-1)}}{a_l} = \alpha \text{ and } a_0 = 1 \quad (6a)$$

$$a_{(l-1)} > a_l \quad (6b)$$

$$\rho_l = \rho_0 a_l^{-1} = \rho_0 \alpha^l \quad (6c)$$

where  $l = 0, \dots, n - 1$  and  $n$  is the total number of levels in the hierarchy. Note that the scale of level  $l$  is inversely proportional to its scale factor  $a_l$ . Eqn. 6a means that the lowest level has the largest scale factor (or equivalently the smallest scale, i.e., smallest spacing between grid cell firing fields) which is equal to 1 and the proportion between consecutive level scale factors ( $a_l$  and  $a_{(l-1)}$ ) is constant ( $\alpha$ ). Eqn. 6b shows that in our model the scale factor progressively decreases (or the scale progressively increases) with higher levels such that the highest level has the biggest scale (or the smallest scaling factor). Thus higher levels in the hierarchy have lower spatial resolution, appearing as large spacing between grid cell firing fields and larger size of grid and place cell firing fields.

**2.4.1. Random Exploration Phase**—During the random exploration phase the animat recruits place cells in a similar way to the single level case described above. We model the place cell recruitment as a Poisson process hence the inter arrival time between two consecutive place cell recruitments follows an exponential distribution with rate parameter  $\lambda$ . The place cell recruitment occurs either when the animat's location does not activate any place cell at any level, i.e., the current location is not represented in the hierarchical map, or when the Poisson process triggers it. Whenever the recruitment is triggered new place cells are formed at levels where no existing place cell is already active. The exploration phase serves the purpose of creating place cell maps of the same environment at different scales (or resolutions) and the place cell recruitment strategy guarantees full coverage of the environment by the top level (lowest resolution) place cell map as seen in Fig. 4b and Fig. 5b.

**2.4.2. Goal Directed Navigation Phase**—The first step of the goal directed navigation phase is to pick a place cell  $\mathbf{p}_{(goal,q)}$  as the animat's goal place cell. Selection of  $\mathbf{p}_{(goal,q)}$  activates its associated reward cell  $\mathbf{r}_{(goal,q)}$ . Activation of reward cell  $\mathbf{r}_{(goal,q)}$  also activates all other reward cells at levels higher than  $q$  that are connected to place cells with firing fields overlapping the firing field of  $\mathbf{p}_{(goal,q)}$ . The spread of reward cell activation upwards in the hierarchy allows the representation of the selected goal location at place cell map levels with lower resolutions. The main idea is to gradually guide the animat towards the original goal place cell  $\mathbf{p}_{(goal,q)}$  starting from the top (lowest resolution) level. After each full scan of look-ahead linear probes the animat should be able to proceed and arrive to the goal place firing field of the next lower level hence allowing the animat to move towards  $\mathbf{p}_{(goal,q)}$  using sequential linear trajectory segments. Let the set of reward cells activated right after selecting  $\mathbf{p}_{(goal,q)}$  be defined as follow:

$$R = \left\{ \mathbf{r}_{(goal,l)} \right\}_{l=q, \dots, n-1} \quad (7)$$

Next all reward cells associated with currently active goal place cells, i.e., goal place cells with firing fields containing animat's current location, are inhibited. If  $\mathbf{r}_{(goal,q)}$  is among the deactivated reward cells then the navigation task ends successfully. Otherwise, the animat performs a full scan of look-ahead linear probes to find the heading that will take it towards the goal place cell of the next lower level with higher resolution. At this point we need to make sure that at least one of the probes will be able to activate the goal place cell of the lower level. This guarantee can be achieved if two conditions are satisfied. The first condition guarantees that the range of probes at level  $l - 1$ , denoted by  $\gamma_{(l-1)}$ , is large

enough to reach the goal place cell of the same level as shown in Fig. 3. We derive the equations to satisfy the two conditions by analyzing a worst case scenario, shown in Fig. 3, where the goal place cells belonging to two consecutive levels of the hierarchy are externally tangent to each other and the animat's physical location (A in Fig. 3) is at the intersection point of the line passing through the centers of both firing fields with the boundary of the larger goal place cell firing field. This configuration is a worst case scenario for probe lengths because the lengths of the linear probes starting from this particular location (A) of the animat and tangent to the smaller place cell firing field are maximal among all linear probes that would start from any other animat location inside the larger place field. Furthermore, the angle between the two linear probes emanating from the animat's location and tangent to the smaller place cell firing field is the maximum that would guarantee intersection of at least one probe with the small firing field when a complete scan of probes is performed. A complete scan of probes involves  $n$  linear probes separated by  $2\pi/n$  degree angles. Based on this geometric analysis the first condition becomes:

$$\gamma_{(l-1)} > \sqrt{(2\rho_l + \rho_{(l-1)})^2 - \rho_{(l-1)}^2} \quad (8)$$

Since the relative scale between consecutive levels is constant as in Eqn. 6a, we can obtain the condition for the probe range at level 0 by simply substituting  $\gamma_{(l-1)}$  by  $\gamma_0\alpha^{l-1}$  and  $\rho_l$  by  $\rho_0\alpha^l$  in Eqn. 8. After algebraic simplifications we obtain:

$$\gamma_0 = 2\rho_0\alpha\sqrt{1+\alpha^{-1}} \quad (9)$$

Eqn. 9 guarantees us that the probe range at any level will be large enough to reach a goal place cell if the probe range at level 0 is chosen accordingly. The second condition concerns the angle between two neighboring probes denoted by  $\beta$ . We have to make sure that  $\beta$  is small enough to guarantee the activation of a goal place cell at some level. After a trigonometric analysis using Fig. 3 and algebraic substitutions and simplifications as in Eqn. 9 we obtain the following relation:

$$\beta < 2\sin^{-1}\left(\frac{\rho_{(l-1)}}{2\rho_l + \rho_{(l-1)}}\right) = 2\sin^{-1}\left(\frac{1}{2\alpha+1}\right) \quad (10)$$

Since Eqn. 10 gives the *maximum* amount of angular separation between neighboring probes guaranteeing goal place cell activation, multiple probes might activate the same goal place cell depending on the actual  $\beta$  value chosen. At this point we can guarantee that at least one of the probes will activate a goal place cell during a full look-ahead trajectory scan if we pick  $\gamma_0$  and  $\beta$  satisfying Eqn. 9 and Eqn. 10. Note that the condition in Eqn. 9 can also be used to calculate the place cell radius  $\rho_0$  given the probe range  $\gamma_0$  and the constant relative scaling  $\alpha$  between place cell map levels or to calculate  $\alpha$  given  $\rho_0$  and  $\gamma_0$ . The same is valid for the condition in Eqn. 10 where  $\alpha$  can be obtained given  $\beta$ . We can, for instance, obtain  $\rho_0$  and  $\alpha$  if a single probe duration is limited to  $\kappa$  and the probe speed is  $v$ . In this case, the range of a single probe at level 0 will be  $\gamma_0 = \kappa v$ . Substituting this into Eqn. 9 we obtain:

$$\kappa v > 2\rho_0\sqrt{\alpha(1+\alpha)} \quad (11)$$

which is a more general form of Eqn. 9. For instance, if we set the scale ratio between consecutive levels  $\alpha$  to 4, the probe velocity  $v$  to 200 cm/s, and the probe duration  $\kappa$  to 0.5 s then Eqn. 11 gives 11.36 as the maximum place cell firing field radius (cm) at the lowest level of the hierarchy  $\rho_0$ .



At this point the animat is ready to perform a full linear look-ahead trajectory scan but with an important modification from the original single level model. Before the full scan all scale factors,  $a_l$ , are set to 1. This change allows the probe speed at level  $l$  to be  $\alpha^l$  ( $\alpha$  is the scale ratio between two consecutive levels as defined in Eqn. 6a) times faster than it is during normal navigation and lets a probe at level  $l$  cover  $\alpha^l$  times longer range than level 0 for the same duration. Furthermore, we can increase the maximum probe range that the animat can cover by adding more levels to the hierarchy while keeping the duration of the full scan constant. Assuming that the noise accumulation is proportional to the duration of a single probe and everything else being equal, this approach can limit the *maximum* amount of noise per probe while increasing the maximum probe range arbitrarily.

Let  $P_{goal}$  be the set of goal place cells activated *after* a full look-ahead trajectory scan and  $C_{goal}$  be the set of probe headings associated with the activated goal place cells in  $P_{goal}$ :

$$P_{goal} = \{p_{(goal,l)}\}_{l=q,\dots,n-1} \quad (12)$$

$$C_{goal} = \{c_{(goal,l)}\}_{l=q,\dots,n-1}$$

where  $c_{(goal,l)}$  is a probe heading that activated goal place cell at level  $l$ . If multiple probes activate the same goal place cell at level  $l$ , the animat picks one of them at random. The next probe heading  $c^*$  to follow towards the goal is the one that activated the goal place cell at the lowest level:

$$c^* = \underset{c_{(goal,l)}}{\operatorname{argmin}} l \quad (13)$$

The animat proceeds along  $c^*$  until it activates another goal place cell by entering its firing field and the whole process starts over again.

### 3. RESULTS

Simulations are performed using MATLAB version R2009b. Simulation time step per single iteration is set to 0.02 seconds. Each place cell in each level receives inputs from three unique grid cells. Each grid cell receives inputs from three persistent spiking cells with frequency ( $f$ ) 7Hz, spiking threshold value ( $s_{thr}$ ) 0.9, and shared factors ( $b_j$ ) are the same for all persistent spiking cells to the same grid cell, but have different values 0.001, 0.002, and 0.004 for the different grid cells projecting to a given place cell. Persistent spiking cells connected to the same grid cell receive bijective inputs from three head direction cells with preferred directions ( $\theta_j$ ) 0, 120, and 240 degrees. Persistent spiking phase offsets ( $\psi_{(i,j)}$ ) depend on the animat's location at the time of place cell recruitment. The head direction cell  $\rightarrow$  persistent spiking cell  $\rightarrow$  grid cell  $\rightarrow$  place cell network using given parameters generate place cell fields with radius ( $\rho_0$ ) 10 cm. We use an animat with first order motion dynamics, i.e., constant speed and no acceleration. The animat's speed is set to 20 cm/s. Parameter/value tuples relevant to the hierarchical model are given in Table 1. We conduct two simulations. For both simulations we assume that the maximum acceptable duration  $\kappa$  for a single probe during a full linear look-ahead trajectory scan is half a second (500 ms). We do not explicitly model noise. The virtual speed  $v$  during a 'single probe is set to 200 cm/s. The probe range at level 0 ( $\gamma_0$ ) then becomes 100 cm. We calculate the parameters for the hierarchical place cell maps using previously explained conditions.

The first simulation is in an open field enclosed by a square wall with 400 cm for each side. The number of levels  $n$  in the place cell hierarchy is 4. The animat starts the simulation from a point close to the lower-right corner of the enclosure. Fig. 4a shows the animat's trajectory after 10 simulated minutes of the exploration phase. Fig. 4b shows the place cell firing fields of each level constructed during the exploration phase. We pick a level 0 place cell close to the top-left corner of the enclosure as goal location. Fig. 4c shows 10 goal-directed navigation phase trajectories each for a separate trial with the same goal place cells. Different trajectories for the same starting point and the goal location are the result of random selection of  $c_{(goal,l)}$  from among multiple probes activating the same goal place cell at level  $l$ . All 10 trials are successful, i.e., the animat reaches the goal location.

For the second simulation we increase the side length of the enclosure 5 times, i.e., 2000 cm. In order to accommodate the increased scale of the environment we add another level ( $n = 5$ ) increasing the maximum probe range. All other parameters are the same as in the first simulation. Fig. 5a shows the trajectory after 30 simulated minutes of the exploration phase. Fig. 5b shows the hierarchical place cell maps and Fig. 5c shows the goal-directed navigation phase trajectories of 10 trials and the goal place cells. All trials are again successful. The hierarchical model presented in this work is able to adapt to a large increase in scale of the environment by the addition of a single level while keeping the maximum allowed single probe time the same.

#### 4. DISCUSSION

We presented an extension to our previous goal-directed navigation model involving the use of different simulated neuron types, i.e., head direction cells, persistent spiking cells, grid cells, place cells, and reward cells to represent a novel environment. After the selection of a goal place cell the animat performs a mental radial sweep around its current location via linear look-ahead trajectory probes and picks the probe heading that activated place cell(s) associated with active reward cell(s). In the original single level model the environment was cognitively represented by homogeneous place cells with the same firing field size. This put a hard constraint on the maximum probe range due to the degrading effects of accumulated noise and there was no guarantee that any of the probes would activate any goal place cell. We relax the probe range restriction of the original model by using a hierarchy of place cell maps each representing the environment at different scales. This approach allows arbitrary extension of the maximum probe range while keeping the duration of a single probe constant and equivalently guaranteeing a predefined level of noise accumulation regardless of the probe range.

In the absence of any sensory information we expect a rapid noise accumulation during a linear look-ahead scan due to inherent neuron signal noise. Consequently, the accumulated noise, especially in the phase space of the velocity controlled oscillators, would significantly degrade the fidelity of a grid cell's spatial tuning. Our assumption is that the noise accumulation can stay below the catastrophic degradation level for some time even in the absence of all stimuli. This assumption is especially realistic when the model involves a network of coupled noisy oscillators (Zilli and Hasselmo, 2010) where the network dynamics help maintain the signal stability even in the presence of high noise levels. During actual movement the network would still accumulate noise but additional sensory inputs, e.g., visual, olfactory, tactile, auditory, and proprioceptive, could be used to correct for the noise accumulation and to reduce uncertainty keeping the signal degradation at acceptable levels. We are currently working on mechanisms to reset the cognitive map network parameters to a previously experienced state when the animat revisits a previously experienced location. While this reset mechanism does not address the noise accumulation

during look-ahead trajectory scan it should help with the problem of “loop-closure” in a biologically inspired way.

The current state of the hierarchical navigation model does not explicitly deal with potential obstacles in the environment as the previous single level did using a reward diffusion process. We are currently investigating ways to improve the hierarchical model to perform successfully in the presence of obstacles. We are also working on extending the hierarchical approach to model the *remapping* phenomenon previously seen during experimental in-vivo recordings.

One of the requirements of our previous work is the existence of a topological connectivity in the reward cell layer allowing the propagation of a reward signal starting from the goal place cell and decaying at each hop from cell to cell generating a gradient. In our new hierarchical model this requirement is no longer necessary. Eliminating the reward signal gradient in our new model comes with the advantage of a simpler model and imposes less physiological constraints.

There is an increasing amount of evidence supporting the hypothesis of representation of space at multiple scales in rats. Recordings from neurons along the dorsal-ventral axis of the entorhinal cortex show grid cell firing fields gradually increasing in size and separation (Hafting et al., 2005; Sargolini et al., 2006; Giocomo et al., 2011). Stensola et al. (2012) show that in a single rat grid cells in the MEC are organized in anatomically layered modules with distinct scale, orientation, asymmetry, and theta-frequency modulation. Interestingly, the clustering of MEC grid cells is of hierarchical nature and the relative increase of spacing between firing fields in neighboring modules varies between rats with an across-population mean of about  $\sqrt{2}$ . The scale increase found experimentally by Stensola et al. (2012) would correspond to parameter  $\alpha$ , the relative scaling between two consecutive layers, in our hierarchical model. Place cells have not been shown to have discrete spatial scales, but they clearly vary their scale at different dorsal to ventral positions within the hippocampus. Brun et al. (2008) reported that the distance between neighbouring firing fields of grid cells increases from around 50 cm at dorsal recording locations to around 3 m at ventral recording locations. In a similar way Kjelstrup et al. (2008) reported that CA3 pyramidal cells show similar scale characteristics as place field diameters increase from less than 1 meter to around 10 meters along the dorsal to ventral hippocampal axis. Taking into account the functional connectivity between the two cortical regions strongly suggests an interplay between the spatial scale representations of place cells and grid cells. Furthermore, it has been postulated that the running speed might be an important factor in the generation of hippocampal multi-scale spatial representations (Maurer et al., 2005).

Any fast sequential activation of spatially tuned neurons with predictive properties for the animals immediate future locations would constitute a good candidate as physiological evidence for look-ahead scans postulated in our models. The relevant physiological data currently includes spiking forward sweep events (Johnson and Redish, 2007; Pfeiffer and Foster, 2013) and sharp wave ripple events (Foster and Wilson, 2006; Davidson et al., 2009; Louie and Wilson, 2001; Jadhav et al., 2012) observed during goal directed spatial tasks. Evidence gathered about the multi-scale spatial representation in rats combined with the phenomenon of spiking sweep events observed during rat waking behaviour at choice points (Johnson and Redish, 2007) and the sweep events towards the rat's immediate and previously visited goal location in a 2 dimensional environment Pfeiffer and Foster (2013) encourages us about the feasibility of our hierarchical model presented here. An immediate prediction of our model is concurrent spiking sweep activity at choice points, similar to the events observed by Johnson and Redish (2007); Pfeiffer and Foster (2013), at different

locations along the dorsal-ventral axis of both entorhinal cortex and hippocampus (specifically the CA3 region).

Recent data has been used to argue against the oscillatory interference model of grid cells (Yartsev et al., 2011; Domnisoru et al., 2013), but our current model does not depend upon a specific mechanism for generation of grid cells. As an alternative, we could use grid cells generated by attractor dynamics. In this case, the animal would sample different head directions and use a tonic velocity input to a grid cell model to sample the linear trajectory in that direction for grid cells of different scales. This would require separate attractor networks with different widths of radial connectivity, as proposed for generation of the discrete spatial scales of different grid cells (Stensola et al., 2012).

The idea to represent a given space at different scales has been extensively exploited in computer science, computer vision, and signal processing communities under the concept of “scale space” (Lindeberg, 1993; Sporring et al., 1997). The “scale space” is a compact and simultaneous representation of a given signal domain at different scales. Each level is usually obtained by passing the original signal through smoothing (low-pass) filters. For instance, in computer vision based object detection the size of the object to be detected is usually unknown a priori. Hence the detection algorithm can be performed at all levels of the “scale space” of a given image to find the unknown size object (Crowley and Sanderson, 1987). The motivation to generate a “scale space” originates from the fact that objects in the real world are usually found at different scales. Hence objects with arbitrary size can be successfully detected by an algorithm running on different levels of the “scale space”. A similar approach can also be found in database and graph theory as “spatial data partitioning” (de Berg et al., 2008). The main idea is to partition and index a spatial data set to optimize the time spent to perform a query at some cost of additional space to store the partitioned space at multiple levels. Trees are the most commonly used data structures to represent the data at multiple levels in a strict hierarchy. While the original data occupies the leaves of the tree, each intermediate node contains information about its sub-tree. Hence when a query is performed efficient retrieval of the relevant data is possible by following an appropriate search starting from the root and visiting intermediate nodes at each level of the tree. Our hierarchical model approach is closely related to the “spatial data partitioning” approach using a balanced tree (de Berg et al., 2008). Levels of the place cell map hierarchy are analogous to the levels of a balanced tree where each node is a place cell. Each node’s firing field intersects with the firing fields of its sub-tree. Hence the root, i.e., the top level, has the lowest spatial resolution and the leaves, i.e., the bottom level, have the highest spatial resolution. The query in our model is the path to the leaf node with an active reward cell starting from root. The purpose of each linear look-ahead trajectory scan is to find the correct node at the next lower level on the path to the goal leaf node. In our current model we do not specifically concern ourselves with neither space nor time optimality of the hierarchy. However, we are currently working on several extensions inspired by graph theory keeping in mind our model’s close relation to computational geometry.

The technical challenge is bridging the spatial representation that autonomous systems use and the spatial representation created by grid cells in the entorhinal cortex and place cells in the hippocampus. Grid cells show stable firing over long time periods (10 min) even in darkness, indicating robust path integration despite the noise inherent in neural systems which is an extremely challenging feature for the state-of-the-art robotic navigation. If the biological mechanisms of grid cells could be implemented in robots they would provide a dramatic advance over current capabilities of autonomous systems. This model is biologically inspired by the response properties of different classes of neurons, but does not yet address the full range of biophysical details in the system. It is a natural tendency to try to imitate nature’s ways of dealing with the navigation problem in synthetic environments

such as robots. However, one-to-one replication of biological mechanisms might not be the best course of action. For instance, humans are very good at visually recognizing locations they have previously been but only if they can successfully recall the relevant memory imprints which rely on a relatively fragile memory system. In contrast robots do not suffer from the memory degradation effects. They are very good at efficient data storage and retrieval up to the capacity of the storage medium they use but are far from being as good as humans to process visual information. Another hurdle on the way to a good navigation model is the noise in the system. If noise accumulation is not corrected for accordingly the error between robot's estimated location and its actual location will reach unacceptable levels pretty quickly. One way of dealing with noise is to reset the robot's internal representation to a known state based on sensory input. This reset based on sensory input is a mission critical problem for robotic SLAM (Simultaneous Localization And Mapping) systems (Bachrach et al., 2012; Fallon et al., 2012; Kaess et al., 2011) which is also known as the *loop closure problem*. This problem directly relates to the ability of recognizing with high fidelity a previously visited location. A similar work to ours addressing the mechanisms of goal directed navigation is by Duff et al. (2011). Their model is mainly rule based where sensory inputs trigger actions and the result of the triggered actions are fed back through the network to reinforce the chain of actions leading to the goal state. One of the main differences between Duff et al. (2011) and our model is the need for multiple trials for the learning rules to converge for a particular goal contingency. When the goal contingency switches, e.g., changing the goal location from left to right arm of a T-maze, the system parameters have to converge to the new fixed point following several trials. Our model, however, is able to perform the goal finding task without the need of additional training trials even if the the goal location changes once the environment's spatial topology is sufficiently acquired. In a recent work Fibla et al. (2010) propose a goal directed navigation model utilizing gradient fields for path planning towards goal locations. In light of these results it might be a better approach to imitate or get inspired by parts of the biological navigation systems that solve or improve their synthetic counterparts.

## References

- Bachrach A, Prentice S, Huang A, Peter H, Krainin M, Maturana D, Fox D, Roy N. Estimation, Planning and Mapping for Autonomous Flight Using an RGB-D Camera in GPS-denied Environments. *International Journal of Robotics Research*. 2012 in press.
- Brown M. Social Influences on Rat Spatial Choice. *Comparative Cognition & Behavior Reviews*. 2011; 6:5–23. URL [http://academicpublishingplatforms.com/downloads/pdfs/ccbr/volume1/201204082211\\_CCBR\\_Vol6\\_2011\\_2.pdf](http://academicpublishingplatforms.com/downloads/pdfs/ccbr/volume1/201204082211_CCBR_Vol6_2011_2.pdf)<http://psyc.queensu.ca/ccbr/Vol6/BrownABS.html>.
- Brun VH, Solstad T, Kjelstrup KB, Fyhn M, Witter MP, Moser EI, Moser M-B. Progressive increase in grid scale from dorsal to ventral medial entorhinal cortex. *Hippocampus*. 2008 Jan; 18(12):1200–1212. URL <http://www.ncbi.nlm.nih.gov/pubmed/19021257>. [PubMed: 19021257]
- Burgess N. Grid cells and theta as oscillatory interference: Theory and predictions. *Hippocampus*. 2008 Dec; 18(12):1157–1174. URL [http://onlinelibrary.wiley.com/doi/10.1002/hipo.20518/abstracthttp://onlinelibrary.wiley.com/store/10.1002/hipo.20518/asset/20518\\_ft.pdf?v=1&t=gulfu2j3&s=6a3a2b0bf71b0ec57bd9bfc9f31318d1c997d76](http://onlinelibrary.wiley.com/doi/10.1002/hipo.20518/abstracthttp://onlinelibrary.wiley.com/store/10.1002/hipo.20518/asset/20518_ft.pdf?v=1&t=gulfu2j3&s=6a3a2b0bf71b0ec57bd9bfc9f31318d1c997d76). [PubMed: 19021256]
- Burgess N, Barry C, O'Keefe J. An oscillatory interference model of grid cell firing. *Hippocampus*. 2007 Sep; 17(9):801–812. URL [http://onlinelibrary.wiley.com/doi/10.1002/hipo.20327/abstracthttp://onlinelibrary.wiley.com/store/10.1002/hipo.20327/asset/20327\\_ft.pdf?v=1&t=gulfuv9q&s=f87210d6b14e07473675aba3cd9e8cde1fe44df1](http://onlinelibrary.wiley.com/doi/10.1002/hipo.20327/abstracthttp://onlinelibrary.wiley.com/store/10.1002/hipo.20327/asset/20327_ft.pdf?v=1&t=gulfuv9q&s=f87210d6b14e07473675aba3cd9e8cde1fe44df1). [PubMed: 17598147]
- Crowley JL, Sanderson AC. Multiple Resolution Representation and Probabilistic Matching of 2-D Gray-Scale Shape. *IEEE Transactions on Pattern Analysis and Machine Intelligence PAMI-9*. 1987 Jan.(1):113–121. URL <http://www.ncbi.nlm.nih.gov/pubmed/21869381http://ieeexplore.ieee.org/lpdocs/epic03/wrapper.htm?arnumber=4767876>.

- Davidson TJ, Kloosterman F, Wilson MA. Hippocampal replay of extended experience. *Neuron*. 2009 Aug; 63(4):497–507. URL <http://www.ncbi.nlm.nih.gov/pubmed/19709631>. [PubMed: 19709631]
- de Berg, M.; Cheong, O.; van Kreveld, M.; Overmars, M. *Computational Geometry: Algorithms and Applications*. 3rd Edition. Springer; 2008.
- Domnisoru C, Kinkhabwala Aa, Tank DW. Membrane potential dynamics of grid cells. *Nature*. 2013 Feb.:1–6. URL <http://www.nature.com/doi/10.1038/nature11973><http://www.ncbi.nlm.nih.gov/pubmed/23395984>.
- Duff A, Sanchez Fibla M, Verschure PFMJ. A biologically based model for the integration of sensorymotor contingencies in rules and plans: A prefrontal cortex based extension of the Distributed Adaptive Control architecture. *Brain Research Bulletin*. 2011 Jun; 85(5):289–304. URL <http://www.sciencedirect.com/science/article/pii/S0361923010002662>. [PubMed: 21138760]
- Egorov AV, Hamam BN, Fransen E, Hasselmo ME, Alonso AA. Graded persistent activity in entorhinal cortex neurons. *Nature*. 2002 Nov; 420(6912):173–178. URL <http://www.ncbi.nlm.nih.gov/pubmed/12432392>. [PubMed: 12432392]
- Erdem UM, Hasselmo ME. A goal-directed spatial navigation model using forward trajectory planning based on grid cells. *The European journal of neuroscience*. 2012 Mar; 35(6):916–931. URL <http://www.ncbi.nlm.nih.gov/pubmed/22393918>. [PubMed: 22393918]
- Eustice RM, Singh H, Leonard JJ. Exactly Sparse Delayed-State Filters for View-Based SLAM. *IEEE Transactions on Robotics*. Dec; 2006 22(6):1100–1114. URL <http://ieeexplore.ieee.org/lpdocs/epic03/wrapper.htm?arnumber=4020357>.
- Fallon MF, Folkesson J, McClelland H, Leonard JJ. Relocating Underwater Features Autonomously Using Sonar-Based SLAM. *IEEE Journal of Oceanic Engineering*. 2012 in press.
- Fibla, M.; Bernardet, U.; Verschure, P. Allostatic control for robot behaviour regulation: An extension to path planning; *Intelligent Robots and Systems (IROS)*, 2010 IEEE/RSJ International Conference on. IEEE; 2010 Oct. p. 1935-1942. URL <http://ieeexplore.ieee.org/ielx5/5639431/5648787/05652866.pdf?tp=\\&arnumber=5652866\\&isnumber=5648787>[http://ieeexplore.ieee.org/xpls/abs\\_all.jsp?arnumber=5652866](http://ieeexplore.ieee.org/xpls/abs_all.jsp?arnumber=5652866)
- Foster DJ, Wilson MA. Reverse replay of behavioural sequences in hippocampal place cells during the awake state. *Nature*. 2006 Mar; 440(7084):680–683. URL <http://dx.doi.org/10.1038/nature04587><http://www.nature.com/nature/journal/v440/n7084/full/nature04587.html><http://www.nature.com/nature/journal/v440/n7084/pdf/nature04587.pdf>. [PubMed: 16474382]
- Fransen E, Tahvildari B, Egorov AV, Hasselmo ME, Alonso Aa. Mechanism of graded persistent cellular activity of entorhinal cortex layer v neurons. *Neuron*. 2006 Mar; 49(5):735–46. URL <http://www.ncbi.nlm.nih.gov/pubmed/16504948>. [PubMed: 16504948]
- Giocomo LM, Hussaini SA, Zheng F, Kandel ER, Moser M-B, Moser EI. Grid cells use HCN1 channels for spatial scaling. *Cell*. 2011 Nov; 147(5):1159–1170. URL <http://www.ncbi.nlm.nih.gov/pubmed/22100643>. [PubMed: 22100643]
- Guanella A, Kiper D, Verschure P. A MODEL OF GRID CELLS BASED ON A TWISTED TORUS TOPOLOGY. *International Journal of Neural Systems*. Aug; 2007 17(04):231–240. URL <http://www.worldscinet.com/ijns/17/1704/S0129065707001093.html>. [PubMed: 17696288]
- Hafting T, Fyhn M, Molden S, Moser M-B, Moser EI. Microstructure of a spatial map in the entorhinal cortex. *Nature*. Aug; 2005 436(7052):801–806. URL <http://dx.doi.org/10.1038/nature03721><http://www.nature.com/nature/journal/v436/n7052/full/nature03721.html><http://www.ncbi.nlm.nih.gov/pubmed/15965463>. [PubMed: 15965463]
- Hasselmo ME. Grid cell mechanisms and function: Contributions of entorhinal persistent spiking and phase resetting. *Hippocampus*. 2008 Dec; 18(12):1213–1229. URL <http://onlinelibrary.wiley.com/doi/10.1002/hipo.20512/abstract>[http://onlinelibrary.wiley.com/store/10.1002/hipo.20512/asset/20512\\_ftn.pdf?v=1\\&t=guljaaq7\\&s=669e3063661c23cda999b62151b64931354affb5](http://onlinelibrary.wiley.com/store/10.1002/hipo.20512/asset/20512_ftn.pdf?v=1\\&t=guljaaq7\\&s=669e3063661c23cda999b62151b64931354affb5). [PubMed: 19021258]
- Hasselmo ME, Stern CE. Mechanisms underlying working memory for novel information. *Trends in cognitive sciences*. 2006 Nov; 10(11):487–493. URL <http://www.pubmedcentral.nih.gov/articlerender.fcgi?artid=2253490\\&tool=pmcentrez\\&rendertype=abstract>. [PubMed: 17015030]

- Jacobs L, Liman E. Grey squirrels remember the locations of buried nuts. *Animal Behaviour*. 1991; 41:103–110. URL <http://www.sciencedirect.com/science/article/pii/S0003347205805068>.
- Jadhav SP, Kemere C, German PW, Frank LM. A wake hippocampal sharp-wave ripples support spatial memory. *Science (New York, N.Y.)*. 2012 Jun; 336(6087):1454–1458. URL <http://www.ncbi.nlm.nih.gov/pubmed/22555434>.
- Johnson A, Redish AD. Neural ensembles in CA3 transiently encode paths forward of the animal at a decision point. *The Journal of neuroscience : the official journal of the Society for Neuroscience*. 2007 Nov; 27(45):12176–12189. URL <http://www.ncbi.nlm.nih.gov/pubmed/17989284>. [PubMed: 17989284]
- Jung MW, Wiener I. Comparison of Spatial Firing Characteristics Ventral Hippocampus of the Rat. *The Journal of Neuroscience*. 1994 Dec.74:7347–7356. [PubMed: 7996180]
- Kaess, M.; Johannsson, H.; Roberts, R.; Ila, V.; Leonard, J.; Dellaert, F. 2011 IEEE International Conference on Robotics and Automation. IEEE; May. 2011 iSAM2: Incremental smoothing and mapping with fluid relinearization and incremental variable reordering; p. 3281–3288. URL <http://ieeexplore.ieee.org/lpdocs/epic03/wrapper.htm?arnumber=5979641>
- Kjelstrup KB, Solstad T, Brun VH, Hafting T, Leutgeb S, Witter MP, Moser EI, Moser M-B. Finite Scale of Spatial Representation in the Hippocampus. *Science*. 2008 Jul; 321(5885):140–143. URL <http://www.sciencemag.org/content/321/5885/140.abstracthttp://www.sciencemag.org/content/321/5885/140.full.pdfhttp://www.sciencemag.org/content/321/5885/140.short>. [PubMed: 18599792]
- Klink R, Alonso A. Muscarinic modulation of the oscillatory and repetitive firing properties of entorhinal cortex layer II neurons. *Journal of neurophysiology*. 1997 Apr; 77(4):1813–1828. URL <http://www.ncbi.nlm.nih.gov/pubmed/9114238>. [PubMed: 9114238]
- Lindeberg, T. *Scale-Space Theory in Computer Vision*. Springer; 1993. URL <http://www.amazon.com/Scale-Space-Computer-Springer-International-Engineering/dp/0792394186>
- Louie K, Wilson M. Temporally structured replay of awake hippocampal ensemble activity during rapid eye movement sleep. *Neuron*. 2001 Jan; 29(1):145–156. URL [http://www.cell.com/neuron/abstract/S0896-6273\(01\)00186-6http://www.sciencedirect.com/science/article/pii/S0896627301001866](http://www.cell.com/neuron/abstract/S0896-6273(01)00186-6http://www.sciencedirect.com/science/article/pii/S0896627301001866). [PubMed: 11182087]
- Maurer AP, Vanrhoads SR, Sutherland GR, Lipa P, McNaughton BL. Self-motion and the origin of differential spatial scaling along the septo-temporal axis of the hippocampus. *Hippocampus*. 2005 Jan; 15(7):841–852. URL <http://www.ncbi.nlm.nih.gov/pubmed/16145692>. [PubMed: 16145692]
- McNaughton B, Barnes C, O'keefe J. The contributions of position, direction, and velocity to single unit activity in the hippocampus of freely-moving rats. *Experimental Brain Research*. 1983 Sep; 52(1):41–49. URL <http://www.springerlink.com/content/t32m405tt7933170/http://www.springerlink.com/index/t32m405tt7933170.pdf>. [PubMed: 6628596]
- Milford, M. 1st Edition. Vol. Vol. 41. Springer Verlag; 2008. Robot navigation from nature: simultaneous localisation, mapping, and path planning based on hippocampal models. URL <http://www.amazon.com/dp/3540775196http://books.google.com/books?hl=en&lr=&id=SwfUZ-teahoC&oi=fnd&pg=PP2&dq=Robot+Navigation+from+Nature:+Simultaneous+Localisation,+Mapping,+and+Path+Planning+Based+on+Hippocampal+Models&ots=n1-iqJdmM&sig=2XYZZEIDT6RAHZCUi9mdBx492c0>
- Milford, M.; Wyeth, G.; Prasser, D. RatSLAM: a hippocampal model for simultaneous localization and mapping. *Robotics and Automation, 2004; Proceedings. ICRA'04. 2004 IEEE International Conference on; IEEE; 2004 May. p. 403-408*. URL [http://ieeexplore.ieee.org/ielx5/9126/29020/01307183.pdf?tp=&arnumber=1307183&isnumber=29020http://ieeexplore.ieee.org/xpls/abs\\_all.jsp?arnumber=1307183](http://ieeexplore.ieee.org/ielx5/9126/29020/01307183.pdf?tp=&arnumber=1307183&isnumber=29020http://ieeexplore.ieee.org/xpls/abs_all.jsp?arnumber=1307183)
- Morris RGM, Garrud P, Rawlins JNP, O'Keefe J. Place navigation impaired in rats with hippocampal lesions. *Nature*. 1982 Jun; 297(5868):681–683. URL <http://dx.doi.org/10.1038/297681a0http://www.nature.com/nature/journal/v297/n5868/abs/297681a0.htmlhttp://www.nature.com/nature/journal/v297/n5868/pdf/297681a0.pdfhttp://www.nature.com/doifinder/10.1038/297681a0>. [PubMed: 7088155]
- Moser EI, Moser M-B. A metric for space. *Hippocampus*. 2008 Jan; 18(12):1142–1156. URL [http://onlinelibrary.wiley.com/doi/10.1002/hipo.20483/abstracthttp://onlinelibrary.wiley.com/store/10.1002/hipo.20483/asset/20483\\_ft.pdf?v=1&t=gulk2fos](http://onlinelibrary.wiley.com/doi/10.1002/hipo.20483/abstracthttp://onlinelibrary.wiley.com/store/10.1002/hipo.20483/asset/20483_ft.pdf?v=1&t=gulk2fos)

\&s=4e3d193ac0f746232db190ca897d95c8eabd6153http://www.ncbi.nlm.nih.gov/pubmed/19021254. [PubMed: 19021254]

- O'Keefe J. Place units in the hippocampus of the freely moving rat. *Experimental Neurology*. 1976 Jan; 51(1):78–109. URL <http://linkinghub.elsevier.com/retrieve/pii/0014488676900558>. [PubMed: 1261644]
- O'Keefe J, Burgess N. Dual phase and rate coding in hippocampal place cells: theoretical significance and relationship to entorhinal grid cells. *Hippocampus*. 2005 Jan; 15(7):853–866. URL <http://www.pubmedcentral.nih.gov/articlerender.fcgi?artid=2677681&tool=pmcentrez&rendertype=abstract>. [PubMed: 16145693]
- O'Keefe J, Burgess N, Donnett JG, Jeffery KJ, Maguire EA. Place cells, navigational accuracy, and the human hippocampus. *Philosophical Transactions of the Royal Society of London. Series B: Biological Sciences*. 1998; 353(1373):1333–1340. URL <http://rstb.royalsocietypublishing.org/content/353/1373/1333.abstract>.
- O'Keefe J, Nadel L. *The hippocampus as a cognitive map*. Oxford: Clarendon Press; 1978. URL [http://www.pdcnet.org/collection/show?id=philstudies1980\\_0027\\_0263\\_0267&pdfname=philstudies\\_1980\\_0027\\_0263\\_0267.pdf&file\\_type=pdf](http://www.pdcnet.org/collection/show?id=philstudies1980_0027_0263_0267&pdfname=philstudies_1980_0027_0263_0267.pdf&file_type=pdf)
- Olton DS, Schlosberg P. Food-searching strategies in young rats: Win-shift predominates over win-stay. *Journal of Comparative and Physiological Psychology*. 1978; 92(4):609–618. URL <http://content.apa.org/journals/com/92/4/609>.
- Pfeiffer BE, Foster DJ. Hippocampal place-cell sequences depict future paths to remembered goals. *Nature*. Apr.2013 URL <http://www.nature.com/doi/10.1038/nature12112>.
- Redish, DA. *Beyond the Cognitive Map*. Cambridge: MIT Press; 1999.
- Sargolini F, Fyhn M, Hafting T, McNaughton BL, Witter MP, Moser M-B, Moser EI. Conjunctive representation of position, direction, and velocity in entorhinal cortex. *Science (New York, N.Y.)*. 2006 May; 312(5774):758–762. URL <http://www.sciencemag.org/content/312/5774/758.shorhttp://www.ncbi.nlm.nih.gov/pubmed/16675704>.
- Schon K, Atri A, Hasselmo ME, Tricarico MD, LoPresti ML, Stern CE. Scopolamine reduces persistent activity related to long-term encoding in the parahippocampal gyrus during delayed matching in humans. *The Journal of neuroscience : the official journal of the Society for Neuroscience*. 2005 Oct; 25(40):9112–9123. URL <http://www.ncbi.nlm.nih.gov/pubmed/16207870>. [PubMed: 16207870]
- Schon K, Hasselmo ME, Lopresti ML, Tricarico MD, Stern CE. Persistence of parahippocampal representation in the absence of stimulus input enhances long-term encoding: a functional magnetic resonance imaging study of subsequent memory after a delayed match-to-sample task. *The Journal of neuroscience : the official journal of the Society for Neuroscience*. 2004 Dec; 24(49):11088–11097. URL <http://www.ncbi.nlm.nih.gov/pubmed/15590925>. [PubMed: 15590925]
- Sharp PE. Multiple Spatial/Behavioral Correlates for Cells in the Rat Postsubiculum: Multiple Regression Analysis and Comparison to Other Hippocampal Areas. *Cerebral Cortex*. 1996 Mar; 6(2):238–259. URL <http://cercor.oxfordjournals.org/content/6/2/238.abstracthttp://cercor.oxfordjournals.org/content/6/2/238>. [PubMed: 8670654]
- Sporring, J.; Nielsen, M.; Florack, L.; Johansen, P. *Gaussian Scale-Space Theory*. Springer; 1997.
- Steele RJ, Morris RGM. Delay-dependent impairment of a matching-to-place task with chronic and intrahippocampal infusion of the NMDA-antagonist D-AP5. *Hippocampus*. 1999 Jan; 9(2):118–136. URL <http://www.ncbi.nlm.nih.gov/pubmed/10226773>. [PubMed: 10226773]
- Steffenach H-A, Witter M, Moser M-B, Moser EI. Spatial Memory in the Rat Requires the Dorsolateral Band of the Entorhinal Cortex. *Neuron*. 2005 Jan; 45(2):301–313. URL <http://www.sciencedirect.com/science/article/pii/S0896627304008542http://www.sciencedirect.com/science?ob=MiamiImageURL&cid=272195&user=489277&pii=S0896627304008542&check=y&origin=&coverDate=20-Jan-2005&view=c&wchp=dGLzVBA-zSkzk&md5=ad3ec3a07f928b161fb6c10fcd9a6dc/1-s2.0-S0896627304008542-main.pdf>. [PubMed: 15664181]



- Stensola H, Stensola T, Solstad T, Frøland K, Moser M-B, Moser EI. The entorhinal grid map is discretized. *Nature*. 2012 Dec; 492(7427):72–78. URL <http://www.ncbi.nlm.nih.gov/pubmed/23222610>. [PubMed: 23222610]
- Suzuki WA, Miller EK, Desimone R. Object and place memory in the macaque entorhinal cortex. *Journal of neurophysiology*. 1997 Aug; 78(2):1062–1081. URL <http://www.ncbi.nlm.nih.gov/pubmed/9307135>. [PubMed: 9307135]
- Tahvildari B, Fransen E, Alonso AA, Hasselmo ME. Switching between “On” and “Off” states of persistent activity in lateral entorhinal layer III neurons. *Hippocampus*. 2007 Jan; 17(4):257–263. URL <http://www.ncbi.nlm.nih.gov/pubmed/17315198>. [PubMed: 17315198]
- Taube J, Muller R, Ranck J. Head-direction cells recorded from the postsubiculum in freely moving rats. I. Description and quantitative analysis. *The Journal of Neuroscience*. 1990 Feb; 10(2):420–435. URL <http://www.jneurosci.org/content/10/2/420.abstract><http://www.jneurosci.org/content/10/2/420.full.pdf>. [PubMed: 2303851]
- Taube JS, Bassett JP. Persistent Neural Activity in Head Direction Cells. *Cerebral Cortex*. 2003 Nov; 13(11):1162–1172. URL <http://cercor.oxfordjournals.org/content/13/11/1162.abstract><http://cercor.oxfordjournals.org/content/13/11/1162.full.pdf>. [PubMed: 14576208]
- Taube JS, Kesslak JP, Cotman CW. Lesions of the rat postsubiculum impair performance on spatial tasks. *Behavioral and neural biology*. 1992 Mar; 57(2):131–143. URL <http://www.ncbi.nlm.nih.gov/pubmed/1586352>. [PubMed: 1586352]
- Yartsev MM, Witter MP, Ulanovsky N. Grid cells without theta oscillations in the entorhinal cortex of bats. *Nature*. 2011 Nov; 479(7371):103–107. URL <http://dx.doi.org/10.1038/nature10583>. [PubMed: 22051680]
- Yoshida M, Fransen E, Hasselmo ME. mGluR-dependent persistent firing in entorhinal cortex layer III neurons. *The European journal of neuroscience*. 2008 Sep; 28(6):1116–1126. URL <http://www.pubmedcentral.nih.gov/articlerender.fcgi?artid=2584367&tool=pmcentrez&rendertype=abstract>. [PubMed: 18783378]
- Young BJ, Otto T, Fox GD, Eichenbaum H. Memory representation within the parahippocampal region. *The Journal of neuroscience: the official journal of the Society for Neuroscience*. 1997 Jul; 17(13):5183–5195. URL <http://www.ncbi.nlm.nih.gov/pubmed/9185556>. [PubMed: 9185556]
- Zilli EA, Hasselmo ME. Coupled noisy spiking neurons as velocity-controlled oscillators in a model of grid cell spatial firing. *The Journal of neuroscience: the official journal of the Society for Neuroscience*. 2010 Oct; 30(41):13850–13860. URL <http://www.jneurosci.org/content/30/41/13850.abstract>. [PubMed: 20943925]

We propose a hierarchical goal directed navigation model based on head direction cells, grid cells, and place cells using look-ahead linear trajectory probes.

We significantly extend our previous work by representing the spatial environment at multiple scales using a hierarchy of place cell maps.

Our hierarchical goal directed navigation model can extend the linear look-ahead probe range arbitrarily while maintaining its duration constant.

Keeping probe duration constant while extending probe range also stabilizes the amount of accumulated noise in the model.

We conduct simulated experiments to show our model's efficacy.

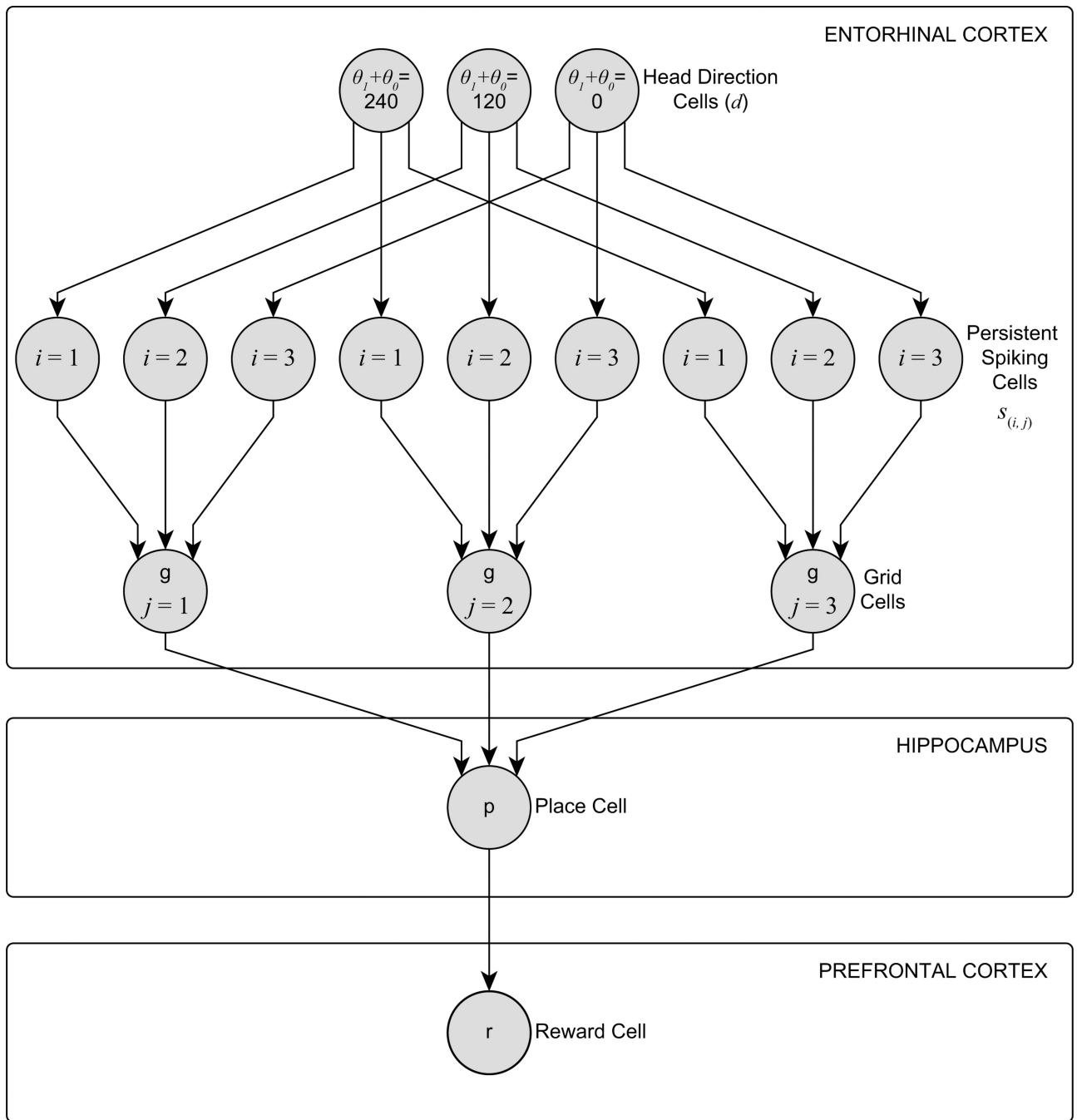


**Figure 1.** The model for head direction cell  $\rightarrow$  persistent spiking cell  $\rightarrow$  grid cell  $\rightarrow$  place cell network.

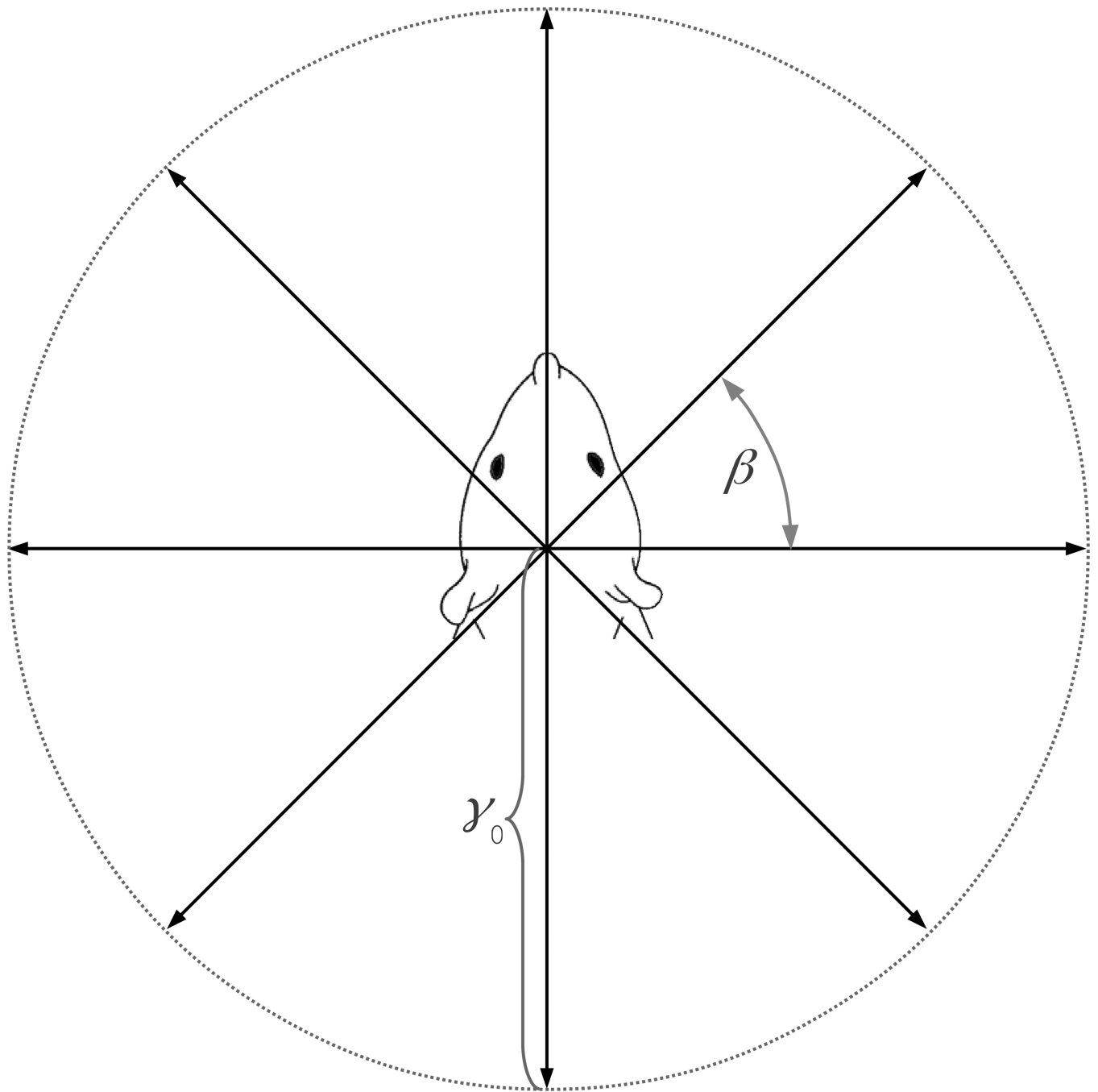


**Figure 2.** Didactic illustration of linear look-ahead trajectory probes for a single level of the place cell map hierarchy. The probe lengths are not shown to scale. The animal does not move while performing a full scan.

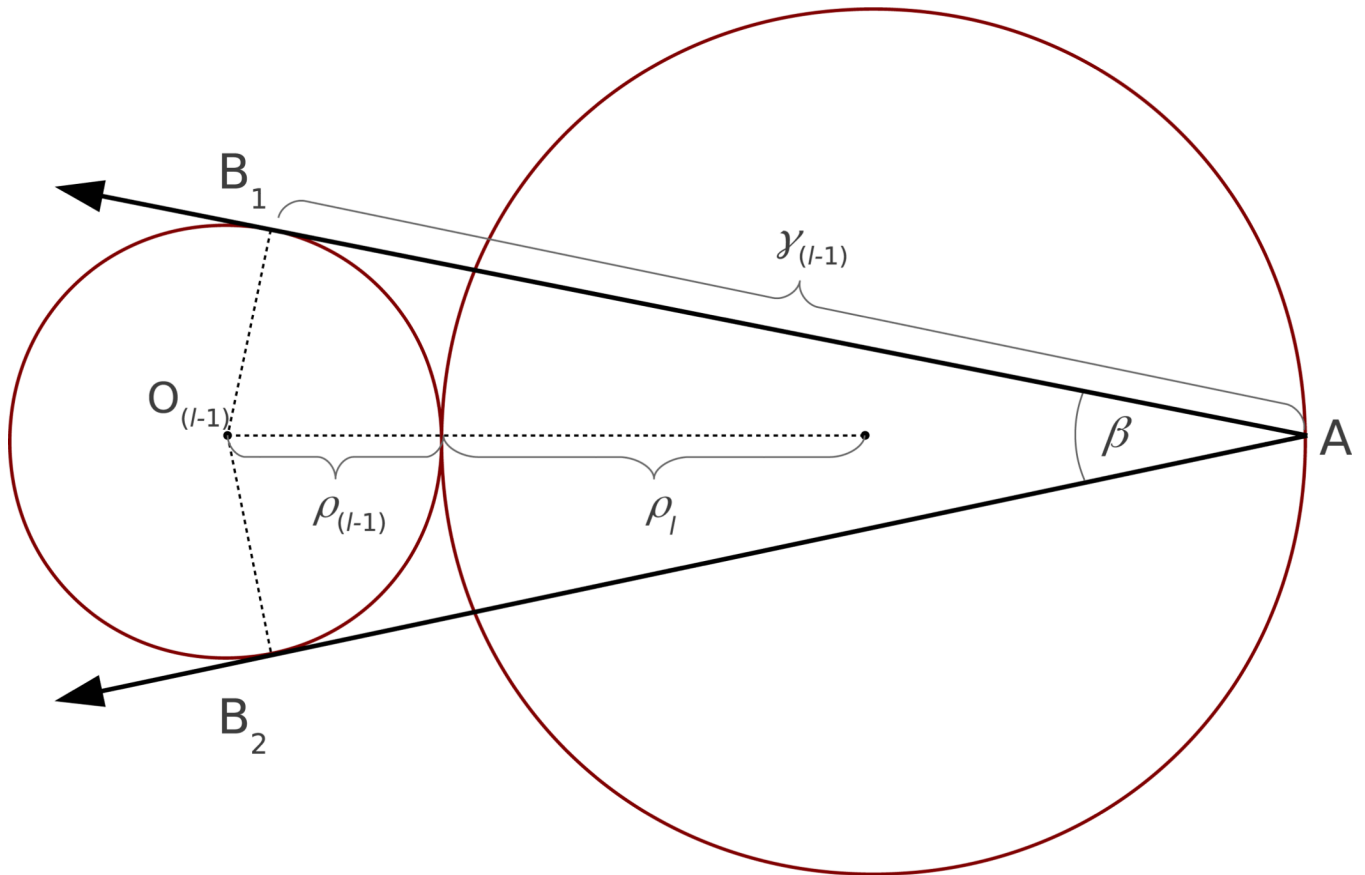


**Figure 3.**

Illustration to explain trigonometric derivation of Eqn. 9 and Eqn. 10. The red circles are the firing fields of two goal place cells  $p_{(l-1)}$  and  $p_l$  from two consecutive levels in the hierarchy. A is the actual location of the animal. The line segments  $\overline{AB_1}$  and  $\overline{AB_2}$  are neighboring probes at level  $l - 1$  and  $|\overline{AB_1}| = |\overline{AB_2}| = \gamma_{(l-1)}$ .  $B_1$  and  $B_2$  are the tangent points between  $p_{(l-1)}$  and the probes. Given that all goal place cell firing fields at different levels of the hierarchy are overlapping by construction, the two tangent firing fields as shown is the worst case scenario for the minimum probe range such that at least one probe at level  $l - 1$  is guaranteed to activate a goal place cell at level  $l - 1$  when the animal is in the firing field of a goal place cell at level  $l$ .

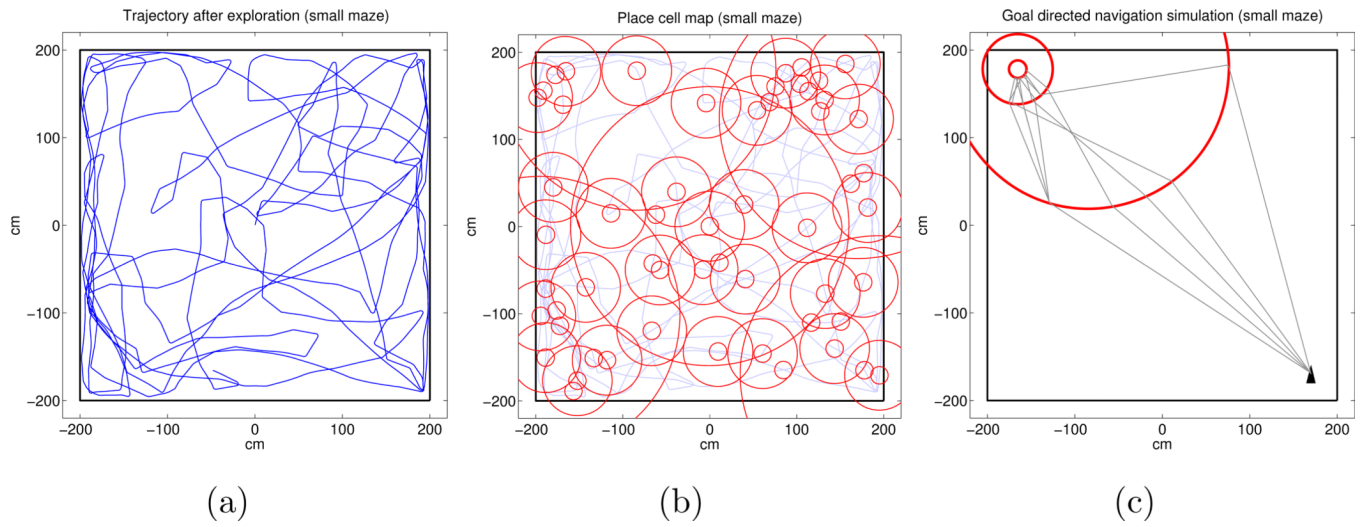


**Figure 4.**  
Simulation 1 results for an open field environment enclosed by a square wall.

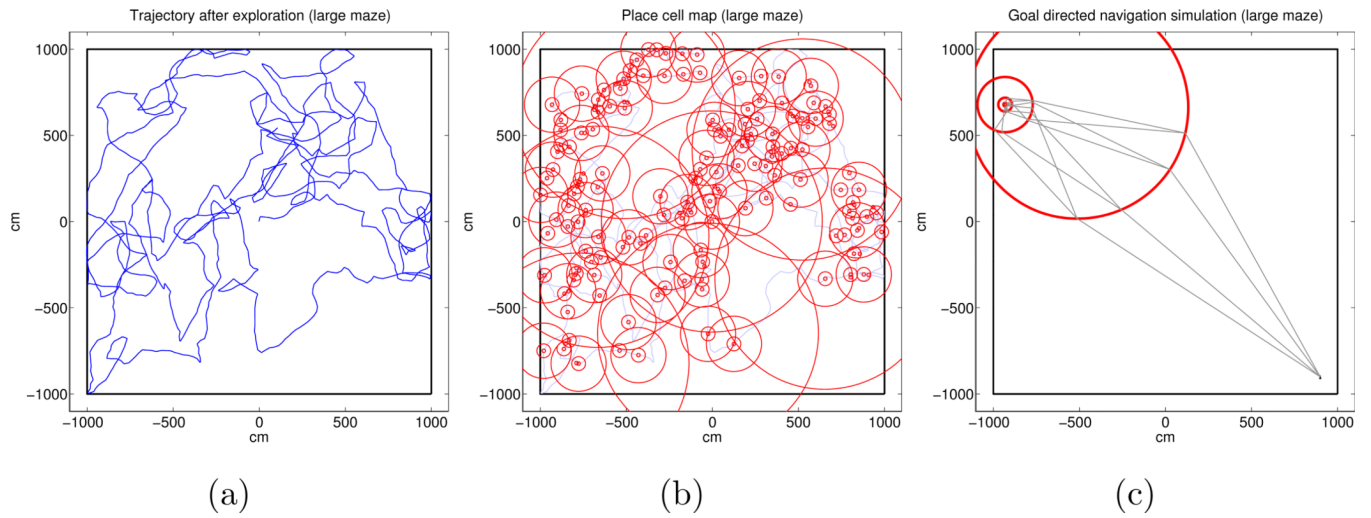


**Figure 5.** Simulation 2 results for an open field environment enclosed by a larger square wall (5 times larger compared to simulation 1).

**Table 1**

Simulation parameters.

Parameter	Value	Parameter	Value
$\alpha$	4	$\lambda$	0.1
$\rho_0$	10 cm	$\gamma_0$	100 cm
$\beta$	7°	$\kappa$	500 ms
$v$	200 cm/s		